LWT - Food Science and Technology 126 (2020) 109281

Contents lists available at ScienceDirect

LWT - Food Science and Technology

journal homepage: www.elsevier.com/locate/lwt

Effects of ethanol on gelation of iota-carrageenan

Dongying Yang[a,b], Hongshun Yang[a,b,*]

[a] Department of Food Science & Technology, National University of Singapore, Singapore, 117542, Singapore
[b] National University of Singapore (Suzhou) Research Institute, 377 Lin Quan Street, Suzhou Industrial Park, Suzhou, Jiangsu, 215123, PR China

ARTICLE INFO

Keywords:
Polysaccharide
Fourier transform infrared (FTIR)
Rheology
Gel
Microstructure

ABSTRACT

The gelation of iota carrageenan (IC) with different ethanol concentrations (0–40 mL/100 mL) was investigated in terms of rheology, chemical structure, and microstructure. Ethanol facilitated IC gel formation with predictable increasing gelling temperature (52.6–62.6 °C) and critical gelling points (50.8–61.3 °C). The ethanol –OH moiety was responsible for Kirkwood-Buff theory through exclusion effects and direct binding with IC. Fourier transform infrared (FTIR) confirmed the binding with the chemical shifts on both sulphated groups (G4S from 850 to 854 cm^{-1} and DA2S from 805 to 808 cm^{-1}). The gel strength decreased at < 10 mL/100 mL ethanol and increased up to 40 mL/100 mL ethanol. From Winter-Chambon equation, 40 mL/100 mL ethanol provided a significantly lower fractal dimension d_f (2.09). Confocal laser scanning microscopy (CLSM) and field emission scanning electron microscopy (FESEM) also showed a less complex network. These results indicated that a small amount of ethanol stabilised IC gelation and that the increased gel strength was more significant at high ethanol concentrations (> 10 mL/100 mL), which improved the design of IC-ethanol systems.

1. Introduction

Carrageenan is a popular food additive for its gelling, stabilising, thickening, and suspending properties from red seaweeds (Huang & Yang, 2019). Carrageenan is ageneric term of different types of linear sulphated galactans according to substitution (sulphation S) diversity. Kappa-carrageenan (KC) and iota-carrageenan (IC) are more frequently used for their gelling potential (Piculell, Nilsson, & Muhrbeck, 1992). They are composed with alternating 3-linked β-D-galactopyranose (G) and 4-linked α-D-galactopyranose (D), as well as the cyclisation form of D units (DA) as disaccharide units. KC with one sulphated group on C_4 of 3-linked β-D-galactopyranose (G4S-DA) and IC with one more sulphated group on C_2 of 4-linked α-D-galactopyranose (G4S-DA2S). Therefore, exert individual rheological properties. Unlike KC, IC tends to produce more elastic gels (Zia et al., 2017). Even though IC is also a popular gelling agent, the mechanism of it differs from KC. Consequently, a better understanding and application of IC gelation would help to expand the spectrum of carrageenan usage.

Carrageenan is water-soluble and commonly works in aqueous systems. However, increased requirements for carrageenan to work in other solvents have appeared. Familiar organic solvents, such as acetone and ethanol, have been reported to be functional in the gelation of KC (Yang, Yang, & Yang, 2018b). As a common alcohol, ethanol has not only to create a favourable alcohol flavour, but is also a crucial precursor in chemistry industry (Sason & Nussinovitch, 2018). For IC, the effect of ethanol on gelation requires further investigation to better collaborate.

The gelation process can be described using rheological tests, which also provide helpful information about food texture, sensory evaluation as well as the performance during mastication and digestion (Alamprese & Mariotti, 2011; Borreani, Hernando, & Quiles, 2020). To better interpret the rheological findings, various mathematical models have been exploited and among them, the power law model (Keogh & O'Kennedy, 1998), the Winter–Chambon model (Winter & Chambon, 1986) and the Kirkwood–Buff (KB) theory (Kirkwood & Buff, 1951) have been applied to express the viscoelastic properties, density, and the interaction between carrageenan and –OH containing molecules.

The goal of this study was to investigate the effect of ethanol addition on chemical structure, microstructure and the rheology of IC using oscillatory rheological tests.

2. Materials and methods

2.1. Materials and sample preparation

Iota carrageenan (IC, Carrageenan Type II) was bought from Merck (St. Louis, MO, USA) as well as fluorescein isothiocyanate (FITC). Potassium bromide (KBr), ethanol (99.9 mL/100 mL), and dimethyl

* Corresponding author. Department of Food Science &Technology, National University of Singapore, Singapore, 117542, Singapore.
E-mail address: fstynghs@nus.edu.sg (H. Yang).

https://doi.org/10.1016/j.lwt.2020.109281
Received 29 December 2019; Received in revised form 12 March 2020; Accepted 13 March 2020
Available online 16 March 2020
0023-6438/

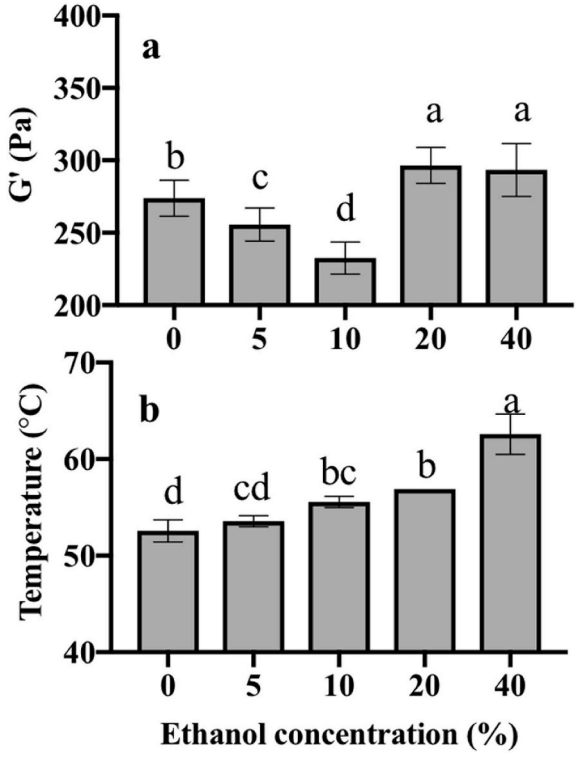

Fig. 1. (a) Gel strength (storage modulus G′ at linear viscosity region) and (b) gelling temperature of 2 g/100 mL iota carrageenan (IC) with 0, 5, 10, 20 and 40 mL/100 mL ethanol. *Within each parameter, means and standard derivations with different lowercase letters were significantly different ($P < 0.05$) among different groups.

sulphoxide (DMSO) were obtained from Merck KGaA (Darmstadt, Germany).

Sunflower oil was bought from a local supermarket in Singapore as cover oil. IC at 2 g/100 mL was prepared (dissolved in hot water first and then mixed with corresponding amount of ethanol), with 0, 5, 10, 20, and 40 mL/100 mL ethanol in DI water.

2.2. Rheological tests

Before the rheological test, sample solutions in section 2.1 were preheated at 90 °C for 60 min with stirring. Then, the plate of a rotational Anton Paar MCR 102 stress-controlled rheometer (Anton Paar, Graz, Austria) with a stainless-steel parallel plate (diameter: 25 mm, gap: 1 mm) was preheated to test the hot solution. Before test started, the sample was covered with plenty of sunflower oil. A series of sweeps were conducted: (a) Angular frequency (1 Hz) and shear strain (1%) were set as constant. Cooling (from 90 °C to 10 °C) and melting (from 10 °C to 90 °C) were measured at the rate of 1 °C/min; (b) The temperature was set at 10 °C for 60 min after cooling to stabilise the gel; (c) Frequency sweep (from 0.1 to 10 Hz) was conducted with shear strain and temperature remaining at 1%, 10 °C from 0.1 to 10 Hz (Ali, Kishimura, & Benjakul, 2018; Yang, Gao, & Yang, 2020). G′ values were used to fit the power law:

$$G' = A\omega^n \quad (1)$$

where ω is the angular frequency (Hz), with known G′ and ω, A can be an indicator of the gel strength, and n is reported to have correlation in the gel;

(d) The other settings remained the same and the shear strain was set to be 0.1–1000%. Upon frature, critical strain can be obtained from the cross point of G′ and G". Before the critical strain, the gel was in linear viscosity region (LVR) (Ramírez-Sucre & Vélez-Ruiz, 2013). The strain sweep produced critical strain (γ_{cr}) as well and it can be used to

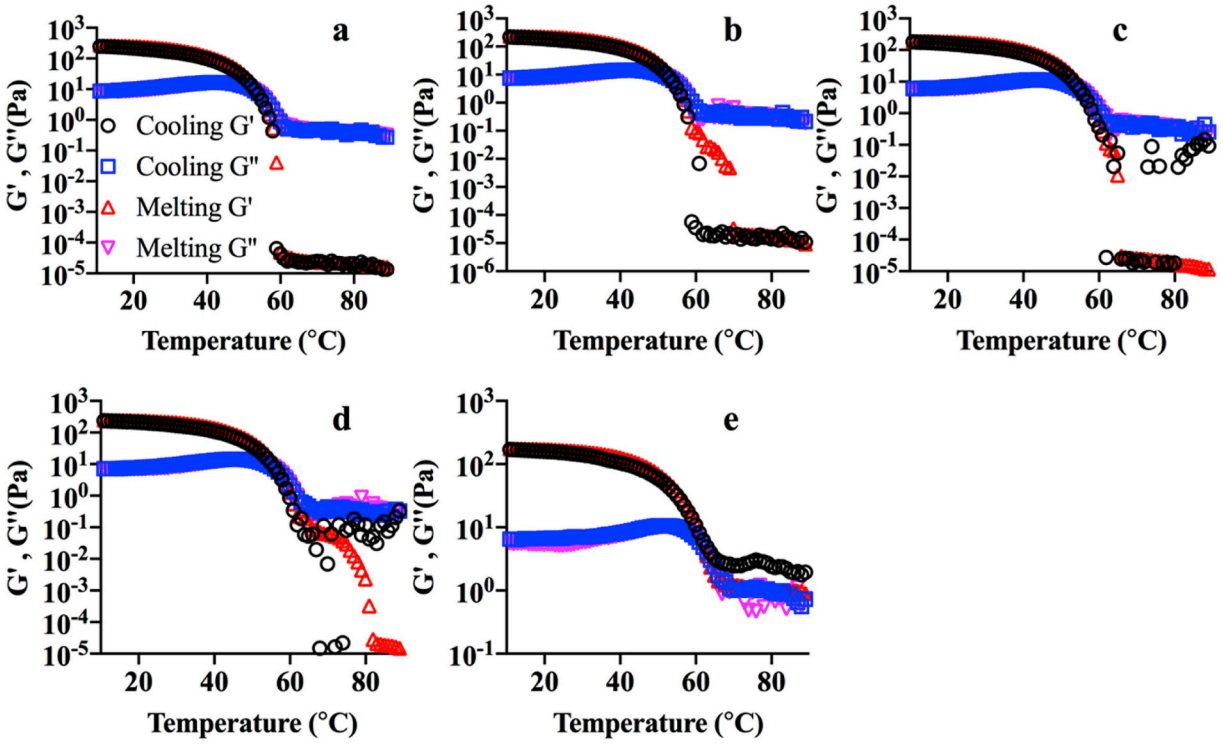

Fig. 2. Dependence of storage modulus G′ and loss modulus G″ as a function of temperature (°C) in cooling and melting sweeps for 2 g/100 mL iota carrageenan (IC) solutions with the addition of ethanol (a) 0, (b) 5, (c) 10, (d) 20, and (e) 40 (mL/100 mL). (○: Cooling G'; □: Cooling G"; △: Melting G'; ▽: Melting G″).

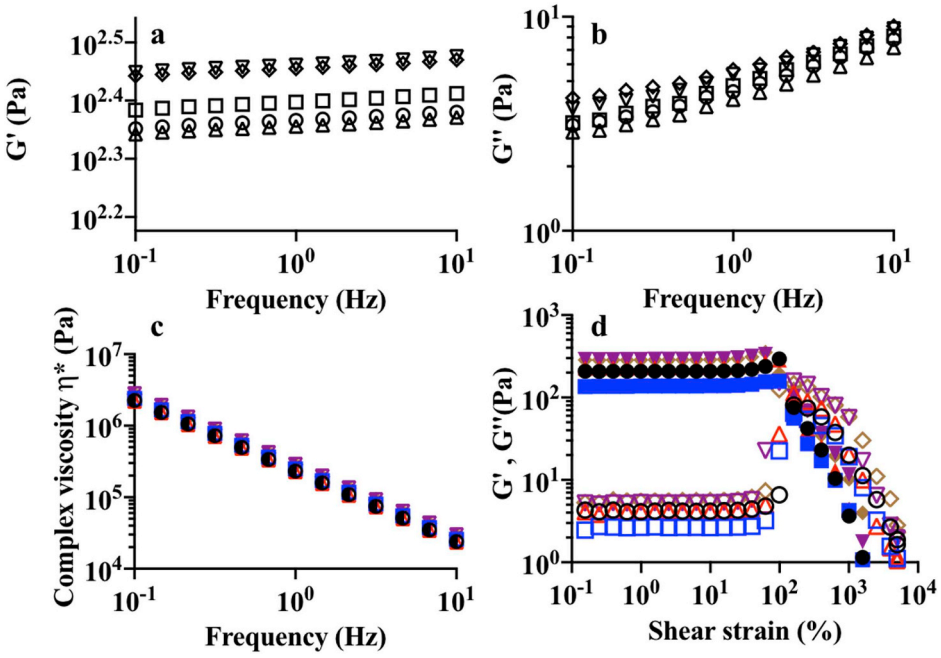

Fig. 3. (a) Storage modulus G′, (b) loss modulus G″ and (c) complex viscosity η* under a frequency sweep, (d) storage modulus G′ under a strain sweep of 2 g/100 mL iota carrageenan (IC) with 0 (○), 5 (□), 10 (△), 20 (▽) and 40 (◇) (mL/100 mL) ethanol.

Table 1
Power Law model fitting, cohesive energy density (E_c) calculation, and Kirkwood-Buff theory calculation of 2 g/100 mL iota carrageenan (IC) with 0, 5, 10, 20 and 40 mL/100 mL ethanol. *Within each row, means with different lowercase letters are significantly different ($P < 0.05$) among different groups.

Composition		0 mL/100 mL	5 mL/100 mL	10 mL/100 mL	20 mL/100 mL	40 mL/100 mL
Power Law	A (10^3 Pa*s$^{(1-n)}$)	2.19 ± 0.19^{b}	2.55 ± 0.71^{ab}	2.68 ± 0.05^{ab}	3.30 ± 0.54^{ab}	3.56 ± 0.99^{a}
	n (10^{-2})	98.8 ± 0.17^{a}	98.7 ± 0.32^{a}	98.9 ± 0.21^{a}	99.0 ± 0.31^{a}	99.0 ± 0.31^{a}
Cohesive energy density (E_c) (J/m^3)		96.36 ± 19.23^{ab}	96.21 ± 22.72^{ab}	106.11 ± 15.97^{a}	68.63 ± 7.97^{b}	76.37 ± 21.08^{ab}
Kirkwood-Buff theory	Melting temperature (T_m) (°C)	53.75 ± 1.5^{d}	55.08 ± 0^{cd}	56.41 ± 0.58^{bc}	57.74 ± 0.57^{b}	63.74 ± 0.58^{a}
	$\Delta T_m/\Delta C$ (K/mol/L)	–	0.22	0.70	0.70	1.19

calculate cohesive energy (E_c) with the relevant storage modulus G′ according to Equation (2).

$$E_C = \int_0^{\gamma_{cr}} G'\gamma_{cr}\delta\gamma = \frac{1}{2}\gamma_{cr}^2 G' \tag{2}$$

(e) Settings in (c) were maintained and temperatures were selected around gelling temperature. Critical gelling points were obtained from the frequency sweeps. The Winter–Chambon equation was then applied to represent the power law relationship among G', G'' and frequency (ω):

$$G'(\omega) \sim G''(\omega) \sim \omega^n \tag{3}$$

in which n, within 0–1, illustrates the elasticity and viscosity of the mixture (Liu & Li, 2016).

Based on the n value, the fractal dimension (d_f) could be calculated using equation (4).

$$n = \frac{d(d+2-2d_f)}{2(d+2-d_f)} \tag{4}$$

where d = 3 was used in the calculation since we were dealing with space dimensions (Rafe & Razavi, 2017).

2.3. Kirkwood–Buff (KB) theory

The KB theory explores the effects of –OH contained co-solvents on gelation (Shimizu & Matubayasi, 2014; Stenner, Matubayasi, & Shimizu, 2016). The calculation is based on the Clausius–Clapeyron equation and KB integrals: ΔG_{u1} (water structural changes) and ΔG_{u2} (cosolvent structural changes) are extracted as shown in equations (5) and (6):

$$\frac{\Delta S_{g\to s}}{RT}\frac{\delta T_{g\to s}}{\delta n_2} = \Delta G_{u1} - \Delta G_{u2} \tag{5}$$

$$\Delta S_{g\to s}\frac{\delta T_{g\to s}}{\delta P} = \Delta V_{g\to s} = -\Delta G_{u1} \tag{6}$$

in these equations, the melting temperature ($T_{g\to s}$) is recorded from sweep (a) and $\delta T_{g\to s}$ can be calculated from pure IC; R is the gas constant; n_2 is the bulk density of ethanol addition; $\Delta S_{g\to s}$ is the entropy change during melting, P is the hydrostatic pressure, $\Delta V_{g\to s}$ represents the volume change during melting and $\Delta S_{g\to s}$, P and $\Delta V_{g\to s}$ can be checked from a previous report (Gekko & Kasuya, 1985; Gekko, Mugishima, & Koga, 1987). ΔG_{u1} calculation based on the parameters mentioned above of pure IC; consequently, it was constant. Furthermore, the value of ΔG_{u2} is directing $\frac{\delta T_{g\to s}}{\delta n_2}$, which can be obtained from rheological test (melting procedure).

2.4. Confocal laser scanning microscopy (CLSM)

IC was stained with FITC (Sow, Nicole Chong, Liao, & Yang, 2018). A stock solution of FITC was first prepared at the concentration of 2 g/100 mL in DMSO. Before mixing, to facilitate binding with FITC, the pH

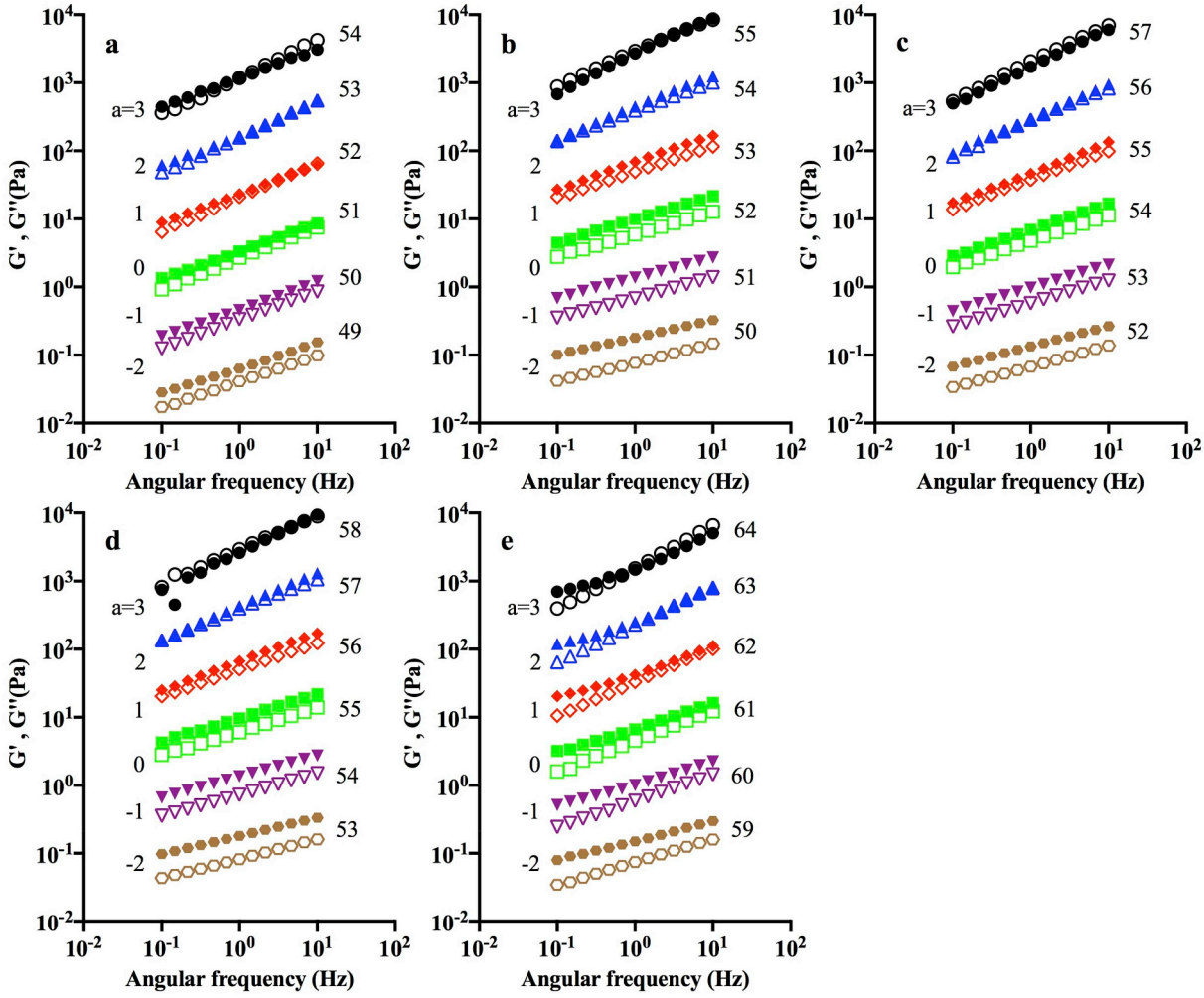

Fig. 4. Dependence of storage modulus G' (solid symbol) and loss modulus G'' (open symbol) as a function of angular frequency (1/s) near gelling temperatures for 2 g/100 mL iota carrageenan (IC) (w/v) solutions with the addition of ethanol (a) 0, (b) 5, (c) 10, (d) 20, and (e) 40 mL/100 mL.

of the IC solution was adjusted to 8.5. Then, 25 μL of dye solution was mixed with 100 mL of the IC solution. Binding was accomplished after 90 min under room temperature. Next, the pH was adjusted back to the original value. Labelled IC was then washed with 95 mL/100 mL ethanol to eliminate redundant FITC and dialysis against DI water. The labelled IC was frozen, dried and again prepared gels with different ethanol concentration (Bui, Nguyen, Nicolai, & Renou, 2019). The mass average molecular weight before ($Mw = 1.2 \times 10^6 g/mol$) and after ($Mw = 5.6 \times 10^5 g/mol$) staining was determined using gel permeation chromatography. This can be a result of one or two covalent bond breakage without altering the rheological properties of IC. Gel state samples (2 g/100 mL) were prepared and 20 μL of the sample was added into a glass well covered with glass slides. Before imaging, the samples were kept in dark at 4 °C overnight. Imaging was conducted on an Olympus Fluoview FV 3000 confocal scanning unit (Tokyo, Japan) with argon ion and Helium–Neon (HeNe) lasers. Images were recorded with water immersion at 60× magnification (PlanApo 60 × /1.0 WLSM 0.17). For FITC, the excitation wavenumber is 495 nm and the emission wavelength is 525 nm. The images were obtained and analysed with ImageJ software (National Institutes of Health, Bethesda, Maryland, USA).

2.5. Field emission scanning electron microscopy (FESEM)

Gel samples from section 2.1 were frozen and dried to produce powder samples for FESEM analysis using a FESEM (JSM-6701F, JEOL, Japan). The samples were pre-freeze in liquid nitrogen to maintain the pores of gel (Hezaveh & Muhamad, 2012). The accelerating rate is 5 kV and at least three representative areas for each sample were scanned.

2.6. Fourier transform infrared (FTIR)

The well-mixed hot samples were cooled down and freeze-dried to obtain dry powder for KBr pellet method. The scanning procedure was taken from Sow, Tan, and Yang (2019): The scanning were all conducted under room temperature and air was scanned as background. Wavenumber from 4000 to 500 cm^{-1} were scanned using a PerkinElmer Spectrum One FTIR spectrometer (PerkinElmer, Waltham, MA, USA) with transmission mode. The recording and processing of spectra were performed with Spectrum software version 6.3.2.

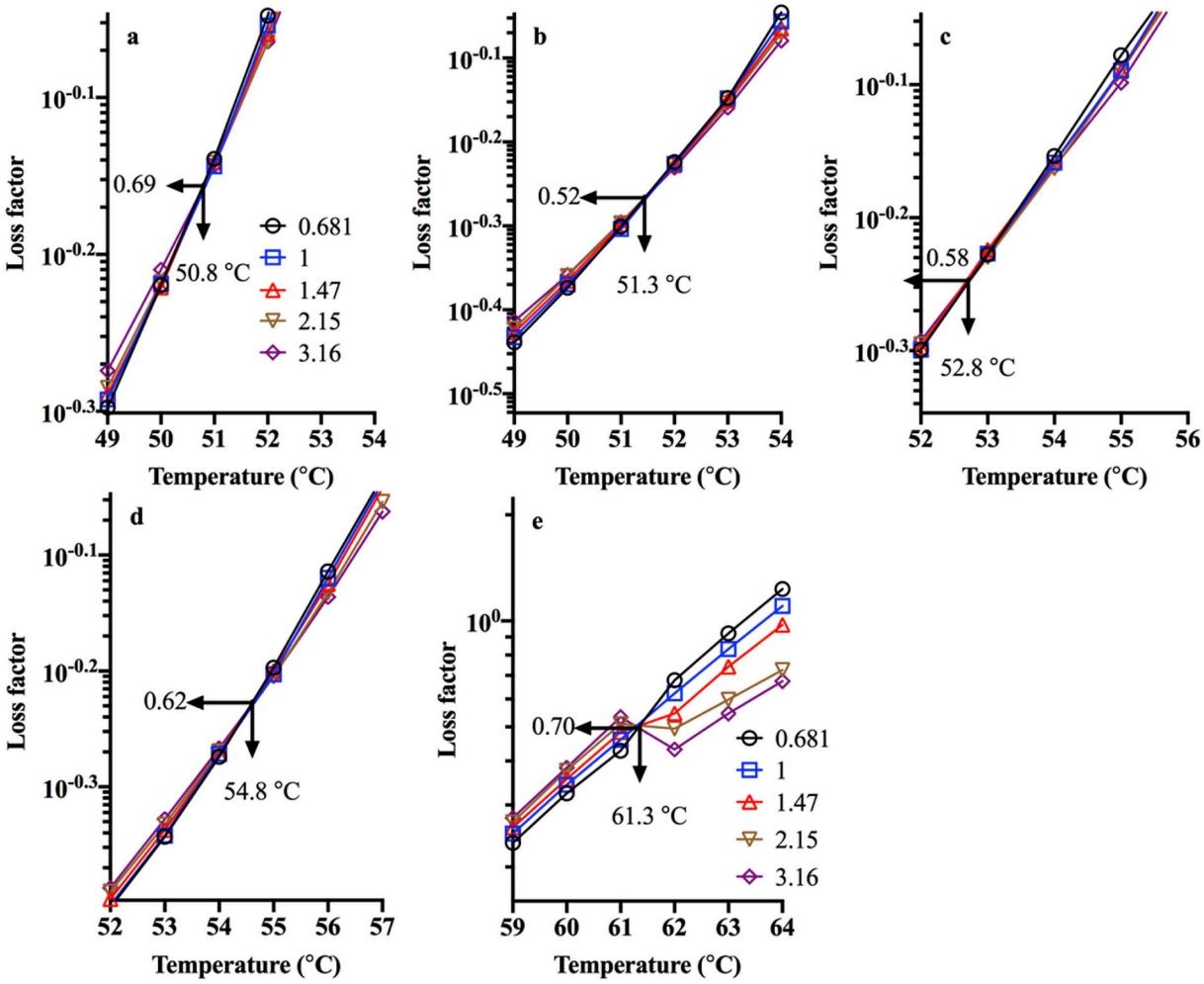

Fig. 5. Dependence of the loss factor as a function of temperature (°C) with different angular frequencies (1/s) for 2 g/100 mL iota carrageenan (IC) solutions with the addition of ethanol at (a) 0, (b) 5, (c) 10, (d) 20, and (e) 40 mL/100 mL. (⊶: 0.681 Hz; ⊟: 1 Hz; ⧋: 1.47Hz; ▽: 2.15 Hz; ◈: 3.15 Hz).

2.7. Statistical analysis

Each test was conducted independently at least three times and the results are expressed as the mean ± the standard deviation (SD). Statistical differences within and between test groups were determined using one-way analysis of variance (ANOVA) ($P < 0.05$) and Student's t-test in the JMP software (SAS, Cary, NC, USA).

3. Results and discussion

3.1. Effect of ethanol on the gelation of IC

Gel strength (G′ of linear viscosity region from frequency sweep) with ethanol concentrations from 0 to 40 mL/100 mL is shown in Fig. 1a. Gel strength reached its low value at mL/100 mL ethanol and increased until 40 mL/100 mL ethanol, while for KC, the gel strength kept going up as a result of increasing junction zones during aggregation (Yang, Yang, & Yang, 2018a). According to the domain model, KC undergoes aggregation while IC does not (Bixler, 2017; Diener et al., 2019). For IC without aggregation procedure, the enhancement effect was accordingly not obvious. Moreover, the swelling effect, which lessened the gel strength, was reported to occur in KC immersing in 30 mL/100 mL ethanol solution (Sason & Nussinovitch, 2018). For IC, there is one more sulphated ester, which may help IC gel better swell in 10 mL/100 mL ethanol solution and consequently reduced the gel strength.

The increase in IC gel strength between 10 and 40 mL/100 mL ethanol might be caused by the hydrophilic property of carrageenan. Carrageenan can be precipitated using an approximately 90 mL/100 mL ethanol solution (Azevedo et al., 2015). Therefore, high concentrations of ethanol facilitate carrageenan assembly via the hydrophobic effect, which overcomes the energy barrier of gelation and stabilise the junction zones (Tkalec, Knez, & Novak, 2015).

Gelling temperature, another critical parameter for monitoring the gelation, kept increasing as shown in Fig. 1b. This confirmed that the addition of ethanol also shifts the equilibrium of IC toward gelation (Stenner et al., 2016).

Cooling and melting curves are shown in Fig. 2. Hysteresis loop has been used to indicate the thermo-reversibility of the gel. Unlike KC, IC experiences little hysteresis because no aggregation occurs (Yuan, Sang, Wang, & Cui, 2018). The addition of ethanol did not seem to change this situation. For IC, in which single helix intertwining forms the

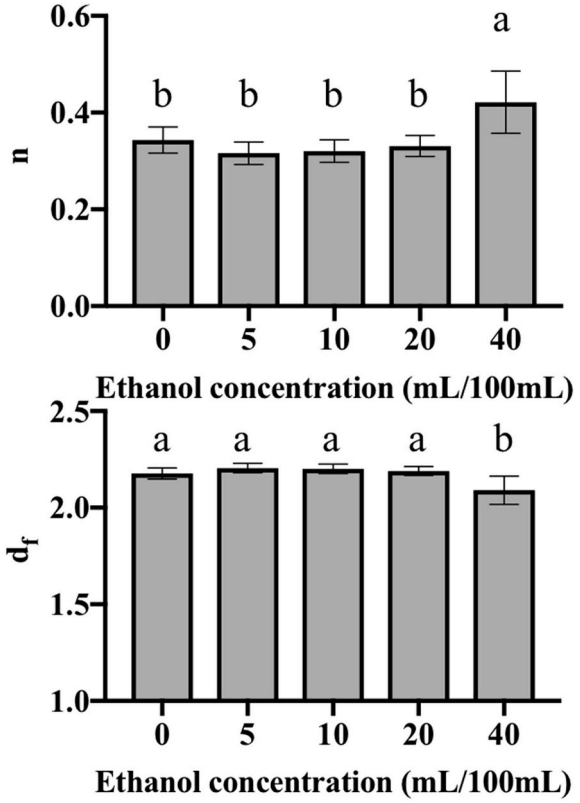

Fig. 6. Dependence of (a) the critical relaxation exponent n and (b) fractal dimension d_f of 2 g/100 mL iota carrageenan (IC) (w/v) solutions with the addition of ethanol at (a) 0, (b) 5, (c) 10, (d) 20, and (e) 40 mL/100 mL.

network and elastic mesh (Diener et al., 2019), the faciliation should be explained with stronger helix intertwining.

3.2. Effect of ethanol on mechanical properties of IC

Frequency sweeps of gels are shown in Fig. 3a–c. G′ and G″ both showed an increasing trend as the frequency increased with less G′ frequent-dependent than G″, indicating a solid-like property (Tau & Gunasekaran, 2016). For η^*, Fig. 3c shows a linear decrease of complex viscosity according to frequency, signifying decreasing mechanical strength. Apart from the shear-thinning behaviour, the value of viscosity also can be an indicator of firmness (Das, Choudhary, & Thompson-Witrick, 2019). Thus, ethanol at more than 10 mL/100 mL could help to decrease the grittiness of IC gels.

The power law model was applied to determine the viscoelastic properties and the fitting results ($R^2 > 0.99$ for all samples) are shown in Table 1. Gel strength can be expressed using pre-exponential factor, *A*. The 40 mL/100 mL ethanol sample had significantly higher gel strength than pure IC. This agreed with the previous findings in section 3.1. Another indicator is the relaxation exponent, *n*, which is positively associated with the rigidity and elasticity of the structure (Wu et al., 2018). All *n* values were close to 1, representing an elastic structure, because when $n = 1$.

Deformation and breaking properties are also critical in the consumption (Chen, Takahashi, Geonzon, Okazaki, & Osako, 2019). The deformation occurred during shear strain increased as shown in Fig. 3d. Initially, G′ and G″ remained independent of shear strain, with G′ being significantly larger than G″ in LVR. After deformation, G′ reduced much more rapi100 mLy than G″ and the crossover points were observed as critical strain. Ethanol addition had little effect on the critical strain. Based on the critical strain, the cohesive energy density (E_c) could be calculated and the results are shown in Table 1. Generally, E_c can reflect certain thermophysical and mechanical properties, such as the elastic modulus and heat capacity (Li & Strachan, 2018).

3.3. Effect of ethanol on critical gelling temperatures of IC according to the Winter–Chambon equation

The critical gelling temperature was determined according to the frequency sweep as shown in Fig. 4. To avoid overlapping, a factor of 10^a was applied to separate the curves. G′ was smaller than G″ before gellling then started to approach G″ as the temperature decreased to the gelling points. Entanglement of polymer branches can cause a plateau in the G′ sweep (Covis et al., 2016). When G′ was larger than G″, there was a gel formed.

The critical gelling temperature could be obtained by the crossover points of loss factor towards the temperature as shown in Fig. 5 since loss factor equals 1 when gelation occurs (Li et al., 2018). The critical gelling temperature increased from 50.8 to 61.3 °C as the ethanol concentration increased, and further confirmed that ethanol promoted IC gelation.

According to the Winter–Chambon equation, the calculated values of n (critical relaxation component) and d_f (fractal dimension) are shown in Fig. 6. As mentioned above, n represents the elasticity of the mixture. Therefore, according to Figs. 6a and 40 mL/100 mL ethanol produced stronger elasticity. This could be explained by more opportunities for helix intertwining (Patel, Campanella, & Janaswamy, 2013). Surprisingly, for d_f (Figs. 6b), 40 mL/100 mL ethanol induced a lower value, indicating less chaotic behaviour and lower complexity of the structures, which is also a reason for increased gel strength (Bi, Li, Wang, & Adhikari, 2017; Kirichenko et al., 2019).

3.4. Evaluation of the mechanisms of the effect of ethanol addition using the KB theory

Melting temperatures and the calculation of $\frac{\delta T_{g\to s}}{\delta n_2}$ are listed in Table 1. The melting temperature increased along with ethanol concentration. Ethanol shifted the equilibrium towards gelation. According to the KB theory, ΔG_{u1} a constant; therefore, $|-\Delta G_{u2}|$ has a positive relationship with $\frac{\delta T_{g\to s}}{\delta n_2}$, representing the contribution of the exclusion effect and direct binding between IC and ethanol. Moreover, $|-\Delta G_{u2}|$ has also been reported to relate to the average amount of –OH (Stenner et al., 2016). As shown in Table 1, the $\frac{\delta T_{g\to s}}{\delta n_2}$ value increased as the ethanol concentration increased. Thus, ethanol facilitated gel formation within the concentration range of 0–40 mL/100 mL by participating in the exclusion effect and binding to IC.

3.5. Microstructure analysis using FESEM

As shown in Fig. 7, IC gels in different concentration of ethanol exhibited different microstructures. IC gels in water behaved as interconnective network as shown in Fig. 7a. 5 mL/100 mL and 10 mL/100 mL ethanol gels presented flexible networks from Fig. 7b & c. When the ethanol concentration increased to 20 mL/100 mL and 40 mL/100 mL, the microstructure became more rigid and denser. It is in agreement with the previous research, which indicated that high ethanol concentration stabilised the intermolecular interactions and

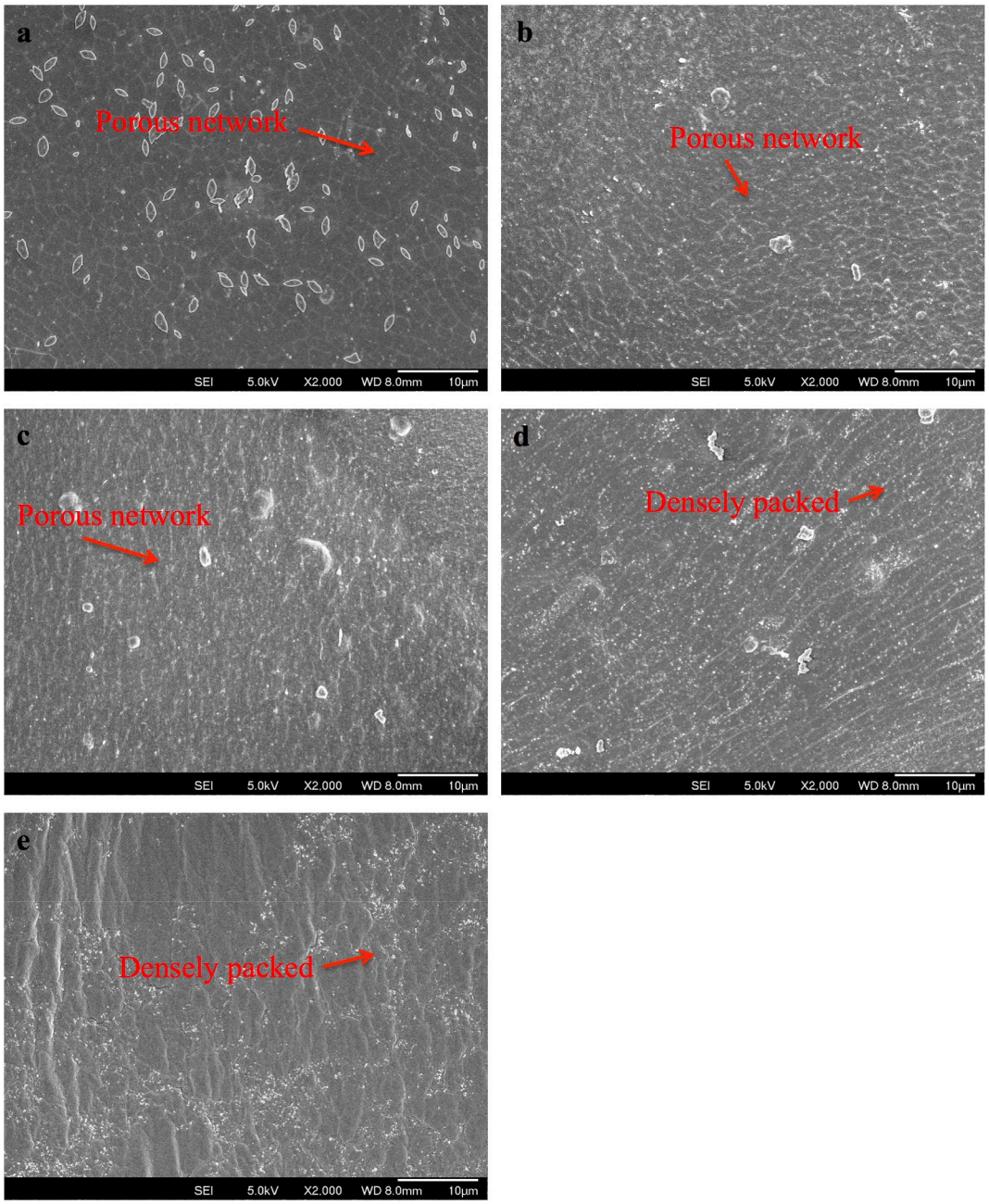

Fig. 7. Field emission scanning electron microscopy (FESEM) images of iota carrageenan (IC) with addition of 0, 5, 10, 20 and 40 mL/100 mL ethanol.

produced dense strands rather than interconnective network of carrageenan (An, Nussio, Huson, Voelcker, & Shapter, 2010; Yang et al., 2018a).

3.6. Interaction between ethanol and IC

FTIR spectra of IC with different ethanol concentration were shown in Fig. 8. Generally speaking, they produce similar spectra (assignments listed in Table 2): A broad band at around 3400 cm^{-1} can be due to O–H stretching in IC; A strong and sharp peak at around 1639 cm^{-1} roots in the glycosidic linkages and O–C–O bond (Sheng et al., 2018); The broad peak at around 1260 cm^{-1} indicates the presence of the sulphate ester in IC; The peaks at about 935 cm^{-1} and 1070 cm^{-1} come from C–O bonds of 3,6-anhydrogalactose (DA); The signals at around 900 cm^{-1} indicates C–O–SO_4 on C_2 of 3,6-anhydrogalactose (DA2S) (Pereira, Amado, Critchley, van de Velde, & Ribeiro-Claro, 2009).

Some peaks illustrate differences upon ethanol addition: The peak at around 805 cm^{-1}, which also responsible for C–O–SO_4 of DA2S, represents a shift to around 808 cm^{-1} and the peak at around 850 cm^{-1} indicating C–O–SO_4 on C_4 of galactose-4- sulphate (G4S) (Pereira, Sousa, Coelho, Amado, & Ribeiro-Claro, 2003) shifts to around 854 cm^{-1}. This variation suggests the interaction between IC and

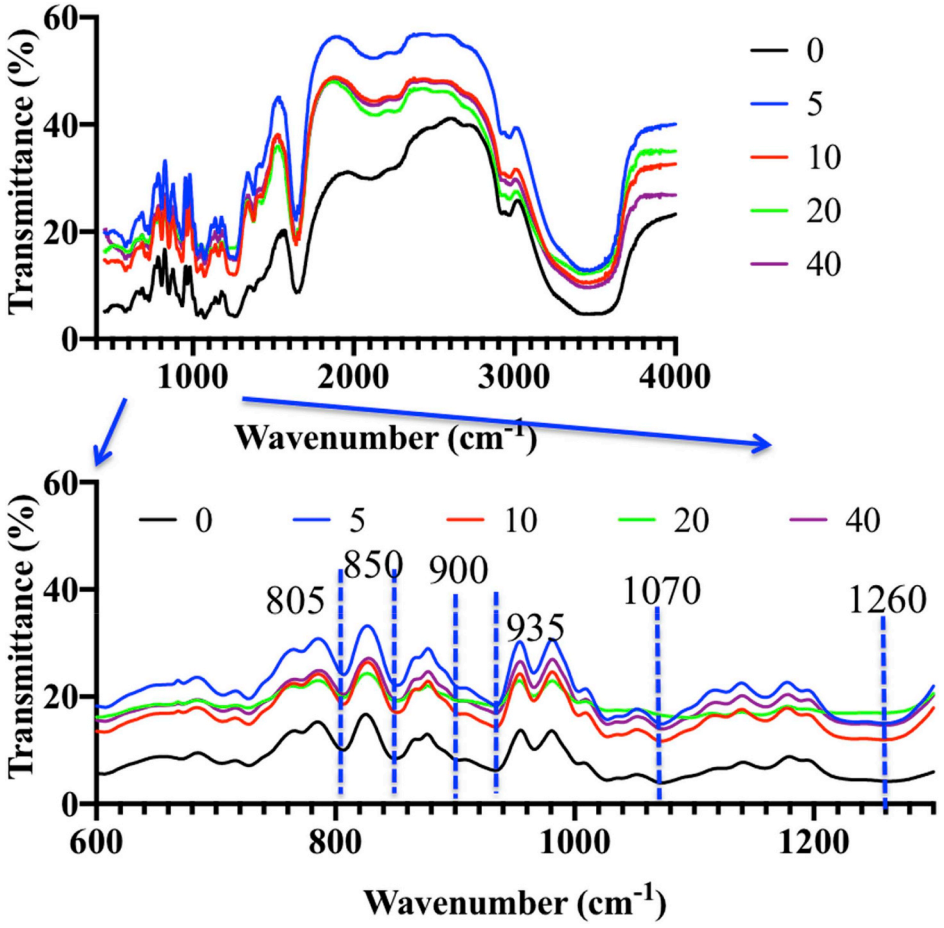

Fig. 8. Fourier transform infrared (FTIR) spectra of iota carrageenan (IC) with addition of 0 (black), 5 (blue), 10 (red), 20 (green) and 40 (purple) mL/100 mL ethanol. (For interpretation of the references to colour in this figure legend, the reader is referred to the Web version of this article.)

Table 2
FTIR peaks location and assignment of 2 g/100 mL iota carrageenan (IC) (w/v) with 0, 5, 10, 20 and 40 mL/100 mL ethanol.

Peak wavenumber (cm^{-1})					Assignments
0 mL/100 mL	5 mL/100 mL	10 mL/100 mL	20 mL/100 mL	40 mL/100 mL	
1260	1260	1260	1260	1260	O = S = O of sulphated esters
935	935	935	935	935	3,6-anhydro-D-galactose (DA)
900	900	900	900	900	C–O–SO_4 on C_2 of 3,6-anhydrogalactose (DA2S)
850	852	854	854	854	C–O–SO_4 on C_4 of galactose-4- sulphate (G4S)
805	808	808	808	808	C–O–SO_4 on C_2 of 3,6-anhydrogalactose (DA2S)

Note that the assignments are taken from previous reports (Pereira et al., 2009; Yang et al., 2018b).

ethanol may happen at the sulphated ester location. Solvent effects and potential for hydrogen bond formation may be the reason for the peak shifts. Ethanol has a smaller contact angle than water, which provide easier contact between ethanol and IC (Bricha & El Mabrouk, 2019).

3.7. Schematic model

A schematic model is presented in Fig. 9. According to rheological tests, both gelling and melting temperatures increased as the ethanol concentration increased, without generating more hysteresis to gelling and melting curves. This could be caused by an equilibrium shift towards gel formation caused by ethanol through the exclusion effect and its binding to IC, referring to the KB theory (Stenner et al., 2016). Ethanol's –OH groups might help the formation of hydrogen bonds with IC to stabilise the gel, while the alkyl groups might increase exclusion because of their hydrophobicity.

Low concentrations of ethanol (< 10 mL/100 mL) seemed to reduce the gel strength. This might be because the better flexibility because a more freely intertwined structure tends to be softer (Diener et al., 2019). Thereafter, up to 40 mL/100 mL ethanol, increasing amounts of

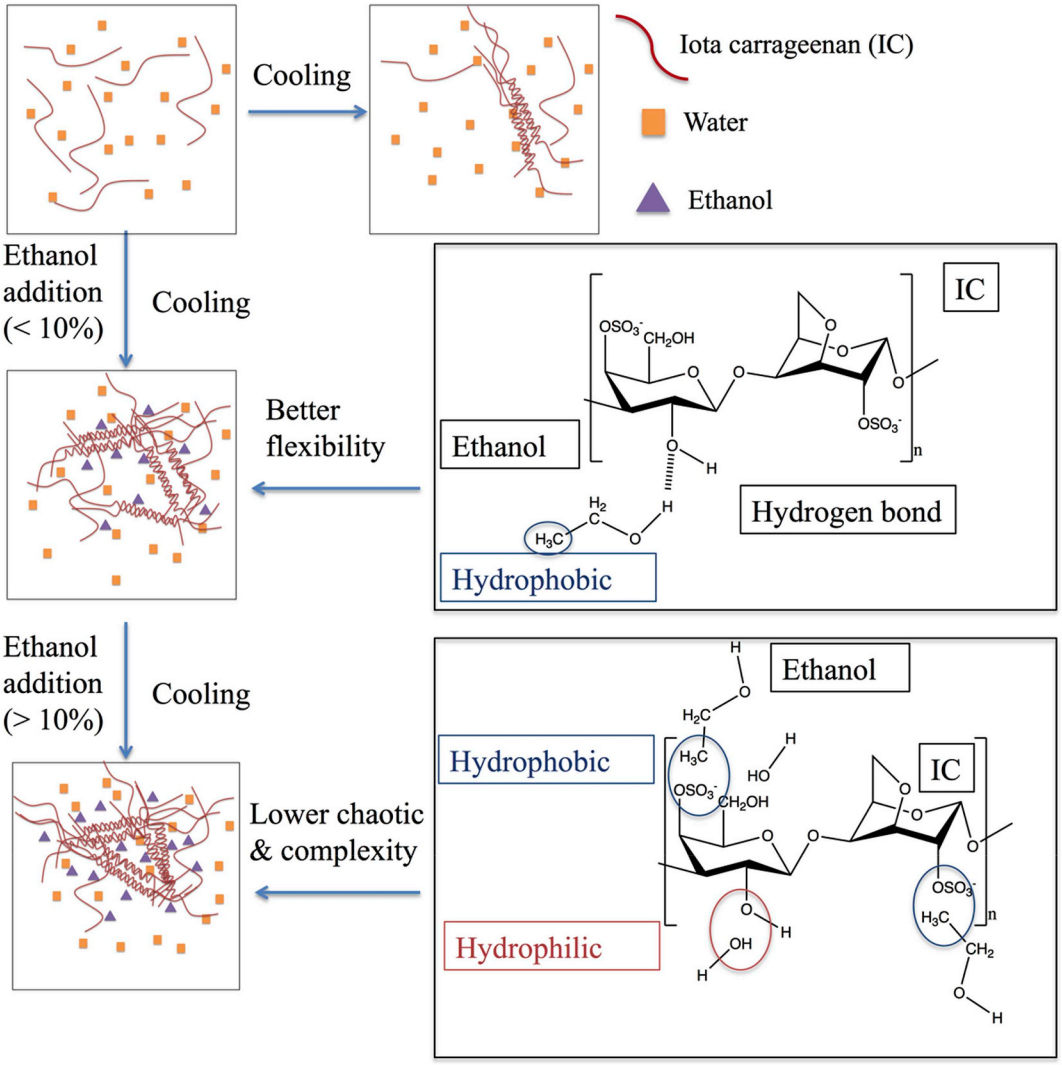

Fig. 9. Schematic presentation of the enhancement effect produced by sucrose on iota carrageenan (IC) gelation: a lower concentration of ethanol (< 10 mL/100 mL) stabilised the gel with –OH group while increased the flexibility and produced softer gel; a higher concentration of ethanol (> 10 mL/100 mL) also stabilised the gel and the hydrophobic effect became dominant to rigi100 mLy arranged IC and produced stronger gels.

ethanol enhanced the gel strength. This was also indicated by the d_f value, which indicated less chaotic behaviour and a less complex structure (Kirichenko et al., 2019). The hydrophobic effect could be the dominant force to better arrange the distribution of IC, leading to a more rigid network.

3.8. Model validation

Microstructures of the gel state samples (2 mL/100 mL w/v) were imaged using CLSM, as shown in Fig. 10. To examine IC through brightness difference, the contrast of the images was not manually adjusted using the same scale. In general, from Fig. 10a–e, all gels exhibited a homogenous connective network with some bright aggregates, as commonly seen in gels (Bui, Nguyen, Renou, et al., 2019). Upon ethanol addition, the microstructure first showed less uniformity up to 10 mL/100 mL ethanol, and then showed better homogeneity up to 40% ethanol. Fig. 10e (40 mL/100 mL ethanol) shows a significantly dense network comparing with the other samples. Together with stabilisation of junction zones, ethanol also helps to push IC molecules closer to each other via the hydrophobic effect. The exclusion of ethanol is believed to be stronger because of its higher number hydrophobic groups (Sason & Nussinovitch, 2018).

4. Conclusion

Ethanol facilitated the gelation of IC with increasing gelling temperature as the ethanol concentration increased. Both –OH groups and hydrophobic groups in ethanol contributed to the enhancement by shifting the equilibrium towards gelation, according to the KB theory. Meanwhile, ethanol addition maintained the gel-forming mechanism as well as the shear-thinning behaviour of IC. For gel strength, ethanol below 10 mL/100 mL reduced it at the expense of better flexibility; ethanol concentrations above 10 mL/100 mL produced increased gel strength as a result of a dominant hydrophobic effect with a more rigid network structure (lower d_f value).

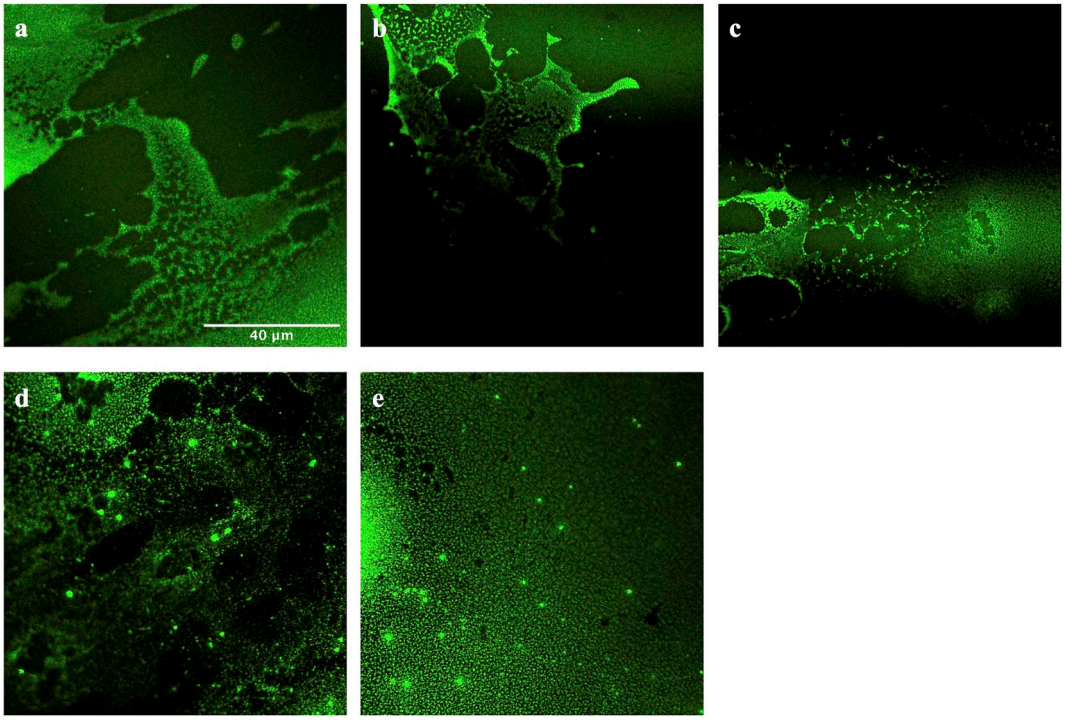

Fig. 10. Microstructure of 2 g/100 mL iota carrageenan (IC) with (a) 0; (b) 5; (c) 10; (d): 20; (e) 40 mL/100 mL ethanol * Fluorescein isothiocyanate (FITC, green) was used to stain the IC. (For interpretation of the references to colour in this figure legend, the reader is referred to the Web version of this article.)

CRediT authorship contribution statement

Dongying Yang: Data curation, Formal analysis, Investigation, Methodology, Resources, Software, Validation, Visualization, Writing - original draft. **Hongshun Yang:** Conceptualization, Funding acquisition, Project administration, Supervision, Writing - review & editing.

Declaration of competing interest

We declare that we have no commercial or associative interest that represents a conflict of interest in connection with this manuscript. We have no financial and personal relationships with other people or organisations that can inappropriately influence our work.

Acknowledgements

This work was funded by the Singapore NRF Industry-IHL Partnership Grant (R-160-000-653-281) and student support (R-160-002-653-281), and an industry project provided by Zhengzhou Bella Biotechnology Co., Ltd (R-160-000-B15-597).

References

Alamprese, C., & Mariotti, M. (2011). Effects of different milk substitutes on pasting, rheological and textural properties of puddings. *Lebensmittel-Wissenschaft und -Technologie- Food Science and Technology, 44*(10), 2019–2025.

Ali, A., Kishimura, H., & Benjakul, S. (2018). Physicochemical and molecular properties of gelatin from skin of golden carp (*Probarbus Jullieni*) as influenced by acid pretreatment and prior-ultrasonication. *Food Hydrocolloids, 82*, 164–172.

An, H., Nussio, M. R., Huson, M. G., Voelcker, N. H., & Shapter, J. G. (2010). Material properties of lipid microdomains: Force-volume imaging study of the effect of cholesterol on lipid microdomain rigidity. *Biophysical Journal, 99*(3), 834–844.

Bi, C., Li, D., Wang, L., & Adhikari, B. (2017). Effect of LBG on the gel properties of acid-induced SPI gels. *LWT- Food Science and Technology, 75*, 1–8.

Bixler, H. J. (2017). The carrageenan controversy. *Journal of Applied Phycology, 29*(5), 2201–2207.

Borreani, J., Hernando, I., & Quiles, A. (2020). Cream replacement by hydrocolloid-stabilized emulsions to reduce fat digestion in *panna cottas*. *LWT- Food Science and Technology, 119*, 108896.

Bricha, M., & El Mabrouk, K. (2019). Effect of surfactants on the degree of dispersion of MWNTs in ethanol solvent. *Colloids and Surfaces A: Physicochemical and Engineering Aspects, 561*, 57–69.

Bui, V., Nguyen, B. T., Nicolai, T., & Renou, F. (2019). Mobility of carrageenan chains in iota- and kappa carrageenan gels. *Colloids and Surfaces A: Physicochemical and Engineering Aspects, 562*, 113–118.

Bui, V., Nguyen, B. T., Renou, F., & Nicolai, T. (2019). Rheology and microstructure of mixtures of iota and kappa-carrageenan. *Food Hydrocolloids, 89*, 180–187.

Chen, C., Takahashi, K., Geonzon, L., Okazaki, E., & Osako, K. (2019). Texture enhancement of salted Alaska pollock (*Theragra chalcogramma*) roe using microbial transglutaminase. *Food Chemistry, 290*, 196–200.

Covis, R., Guegan, J. P., Jeftić, J., Czjzek, M., Benoit, M., & Benvegnu, T. (2016). Structural and rheological properties of kappa (κ)-carrageenans covalently modified with cationic moieties. *Journal of Polymer Research, 23*(4), 78.

Das, K., Choudhary, R., & Thompson-Witrick, K. A. (2019). Effects of new technology on the current manufacturing process of yogurt-to increase the overall marketability of yogurt. *LWT- Food Science and Technology, 108*, 69–80.

Diener, M., Adamcik, J., Sánchez-Ferrer, A., Jaedig, F., Schefer, L., & Mezzenga, R. (2019). Primary, secondary, tertiary and quaternary structure levels in linear polysaccharides: From random coil, to single helix to supramolecular assembly. *Biomacromolecules, 20*(4), 1731–1739.

Gekko, K., & Kasuya, K. (1985). Effect of pressure on the sol-gel transition of carrageenans. *International Journal of Biological Macromolecules, 7*(5), 299–306.

Gekko, K., Mugishima, H., & Koga, S. (1987). Effects of sugars and polyols on the sol-gel transition of κ-carrageenan: Calorimetric study. *International Journal of Biological Macromolecules, 9*(3), 146–152.

Hezaveh, H., & Muhamad, I. I. (2012). The effect of nanoparticles on gastrointestinal release from modified κ-carrageenan nanocomposite hydrogels. *Carbohydrate Polymers, 89*(1), 138–145.

Huang, M., & Yang, H. (2019). Eucheuma powder as a partial flour replacement and its effect on the properties of sponge cake. *LWT- Food Science and Technology, 110*, 262–268.

Keogh, M. K., & O'Kennedy, B. T. (1998). Rheology of stirred yogurt as affected by added milk fat, protein and hydrocolloids. *Journal of Food Science, 63*(1), 108–112.

Kirichenko, M. N., Chaikov, L. L., Krivokhizha, S. V., Kirichenko, A. S., Bulychev, N. A., & Kazaryan, M. A. (2019). Effect of iron oxide nanoparticles on fibrin gel formation and its fractal dimension. *The Journal of Chemical Physics, 150*(15), 155103.

Kirkwood, J. G., & Buff, F. P. (1951). The statistical mechanical theory of solutions. I. *The Journal Of Chemical Physics, 19*(6), 774–777.

Li, Z., Liu, J., Zhang, Z., Gao, Y., Liu, L., Zhang, L., et al. (2018). Molecular dynamics simulation of the viscoelasticity of polymer nanocomposites under oscillatory shear: Effect of interfacial chemical coupling. *RSC Advances, 8*(15), 8141–8151.

Li, C., & Strachan, A. (2018). Cohesive energy density and solubility parameter evolution during the curing of thermoset. *Polymer, 135*, 162–170.

Liu, S., & Li, L. (2016). Thermoreversible gelation and scaling behavior of Ca2+-induced κ-carrageenan hydrogels. *Food Hydrocolloids, 61*, 793–800.

Patel, B. K., Campanella, O. H., & Janaswamy, S. (2013). Impact of urea on the three-dimensional structure, viscoelastic and thermal behavior of iota-carrageenan.

Carbohydrate Polymers, 92(2), 1873–1879.
Pereira, L., Amado, A. M., Critchley, A. T., van de Velde, F., & Ribeiro-Claro, P. J. A. (2009). Identification of selected seaweed polysaccharides (phycocolloids) by vibrational spectroscopy (FTIR-ATR and FT-Raman). *Food Hydrocolloids, 23*(7), 1903–1909.
Pereira, L., Sousa, A., Coelho, H., Amado, A. M., & Ribeiro-Claro, P. J. A. (2003). Use of FTIR, FT-Raman and 13C-NMR spectroscopy for identification of some seaweed phycocolloids. *Biomolecular Engineering, 20*(4), 223–228.
Piculell, L., Nilsson, S., & Muhrbeck, P. (1992). Effects of small amounts of kappa-carrageenan on the rheology of aqueous iota-carrageenan. *Carbohydrate Polymers, 18*(3), 199–208.
Rafe, A., & Razavi, S. M. A. (2017). Scaling law, fractal analysis and rheological characteristics of physical gels cross-linked with sodium trimetaphosphate. *Food Hydrocolloids, 62*, 58–65.
Ramírez-Sucre, M. O., & Vélez-Ruiz, J. F. (2013). Physicochemical, rheological and stability characterization of a caramel flavored yogurt. *Lebensmittel-Wissenschaft und -Technologie- Food Science and Technology, 51*(1), 233–241.
Sason, G., & Nussinovitch, A. (2018). Characterization of κ-carrageenan gels immersed in ethanol solutions. *Food Hydrocolloids, 79*, 136–144.
Sheng, L., Li, P., Wu, H., Liu, Y., Han, K., Gouda, M., et al. (2018). Tapioca starch-pullulan interaction during gelation and retrogradation. *LWT- Food Science and Technology, 96*, 432–438.
Shimizu, S., & Matubayasi, N. (2014). Gelation: The role of sugars and polyols on gelatin and agarose. *The Journal of Physical Chemistry B, 118*(46), 13210–13216.
Sow, L. C., Chong, J. M. N., Liao, Q. X., & Yang, H. (2018). Effects of κ-carrageenan on the structure and rheological properties of fish gelatin. *Journal of Food Engineering, 239*, 92–103.
Sow, L. C., Tan, S. J., & Yang, H. (2019). Rheological properties and structure modification in liquid and gel of tilapia skin gelatin by the addition of low acyl gellan. *Food Hydrocolloids, 90*, 9–18.
Stenner, R., Matubayasi, N., & Shimizu, S. (2016). Gelation of carrageenan: Effects of sugars and polyols. *Food Hydrocolloids, 54*, 284–292.
Tau, T., & Gunasekaran, S. (2016). Thermorheological evaluation of gelation of gelatin with sugar substitutes. *Lebensmittel-Wissenschaft und -Technologie- Food Science and Technology, 69*, 570–578.
Tkalec, G., Knez, Ž., & Novak, Z. (2015). Formation of polysaccharide aerogels in ethanol. *RSC Advances, 5*(94), 77362–77371.
Winter, H. H., & Chambon, F. (1986). Analysis of linear viscoelasticity of a crosslinking polymer at the gel point. *Journal of Rheology, 30*(2), 367–382.
Wu, Y., Guo, R., Cao, N., Sun, X., Sui, Z., & Guo, Q. (2018). A systematical rheological study of polysaccharide from *Sophora alopecuroides* L. seeds. *Carbohydrate Polymers, 180*, 63–71.
Yang, D., Gao, S., & Yang, H. (2020). Effects of sucrose addition on the rheology and structure of iota-carrageenan. *Food Hydrocolloids, 99*, 105317.
Yang, Z., Yang, H., & Yang, H. (2018a). Characterisation of rheology and microstructures of κ-carrageenan in ethanol-water mixtures. *Food Research International, 107*, 738–746.
Yang, Z., Yang, H., & Yang, H. (2018b). Effects of sucrose addition on the rheology and microstructure of κ-carrageenan gel. *Food Hydrocolloids, 75*, 164–173.
Yuan, C., Sang, L., Wang, Y., & Cui, B. (2018). Influence of cyclodextrins on the gel properties of kappa-carrageenan. *Food Chemistry, 266*, 545–550.
Zia, K. M., Tabasum, S., Nasif, M., Sultan, N., Aslam, N., Noreen, A., et al. (2017). A review on synthesis, properties and applications of natural polymer based carrageenan blends and composites. *International Journal of Biological Macromolecules, 96*, 282–301.